NOTES

Limnol. Oceanogr., 43(2), 1998, 334–339

Denitrification in estuarine sediments determined by membrane inlet mass spectrometry

Abstract—Steady-state and transient-state denitrification rates were measured in sediment cores from a brackish river of the Chesapeake Bay using high-precision, membrane-inlet mass spectrometry. Denitrification was independent of salinity over the range of 1–13 ppt and was directly dependent on nitrate concentration over the range of 0–200 μM in the overlying water. Denitrification was observed when the water-column nitrate concentration was <1 μM, indicating that nitrification in the sediments was occurring. There was no detectable lag in the response of denitrification to an abrupt increase in nitrate in the overlying water column; moreover, the enhanced rate under nitrate enrichment was either stable or changed slowly over periods of days. Thus, the microbial flora remained poised to utilize increased nitrate supplies, suggesting that the denitrifiers were facultative. An analysis based on diffusion theory supports a view that denitrification was controlled by properties that affected the physical transport of nitrate from the water to the sites of denitrification. Our results indicate that denitrification in this river can respond rapidly and directly to episodic events that cause changes in water-column nitrate concentration.

Estuarine denitrification is under complex environmental control owing to diverse physical, chemical, and biological factors that affect it both directly and indirectly. Direct (microbe level) effects on the process include substrate (nitrate) availability, oxygen inhibition, organic matter supply, and temperature (Seitzinger 1988; Rysgaard et al. 1994). In nature, these factors are affected by advective and diffusive properties of the estuary that affect transport of materials, or by the influence of separate microbial processes that generate nitrate or affect oxygen tension near the denitrifying bacteria (Nielsen et al. 1995). At the ecosystem scale, denitrification is influenced by seasonality of physical and chemical factors, hydrodynamics of the system, organic cycling, and anthropogenic effects on nutrient loading (Kemp et al. 1990).

This conceptual, if not real, complexity of environmental controls over denitrification is exacerbated by difficulties in measuring the denitrification process (Seitzinger et al. 1993). Direct measurement of denitrification is best done through the measurement of the end product, N_2, but this is difficult because of the high background concentration of the gas. Consequently, N_2 flux studies are often prolonged or the sample is subjected to significant manipulation. Hence, fundamental temporal and substrate-level kinetics of the process that would be useful in modeling and understanding denitrification in situ have been difficult to obtain. We herein describe an application of membrane-inlet mass spectrometry for measuring small changes in dissolved N_2 associated with denitrification in sediments. An advantage of this technique is the ability to measure N_2 fluxes in unperturbed cores with high temporal resolution. This capability has allowed us to address the issues of temporal and substrate-level responsiveness of sediments to changes in nitrate.

Of particular interest was the summertime situation when water-column nitrate concentration is seasonally low and temperature is high. Denitrification in such systems is likely supported principally by coupled nitrification–denitrification at a level below that which could be supported by direct nitrate supply typical of winter or spring conditions (Jenkins and Kemp 1984; Kemp et al. 1990). Given the warmer temperature of summer, the potential for high rates of denitrification is great if nitrate appears in the system. Such loading may occur locally by point-source discharge or regionally by episodic weather events such as wind-driven mixing or freshwater inputs that affect transport of material and nutrients from the shore. The extent to which denitrification responds to such episodic changes will be determined by the response time of the microbial flora and the efficiency of the flora in utilizing nitrate from the environment. To obtain this information, we combined continuous-flow chamber methodology, which allowed us to measure steady-state and transient-state fluxes, with a novel high-precision method of measuring dissolved N_2.

Bottom sediment (silty clay) was sampled from four tidal sites along a salinity gradient (1–14 ppt) in the Choptank River, a tributary of the Chesapeake Bay. Sediment was collected from the aphotic zone at a depth of ~3 m using an acrylic/PVC box corer. The box core was immediately subcored to a depth of 15–20 cm by using 30 × 10.2-cm PVC cylinders. The cores were returned to the laboratory and plumbed for continuous flow within 6 h of initial collection. Sediments were maintained in darkness except during sample periods. Supply water for the flow experiments was collected from the respective site, filtered through 64-μm Nitex netting, and maintained at constant temperature with bubbling in darkened reservoirs.

For each site, triplicate cores plus a sediment-free blank chamber were supplied from a common reservoir with flow-through site water. Incubations were conducted in darkness in a temperature-controlled environment room set at a temperature close to the ambient river water. The water overlying the core, which constituted ~50% of the cylinder volume, was stirred by a magnet at 75 rpm. The flow rate was set at ~3 ml min^{-1} using a Rainin Rabbit peristaltic pump. This flow resulted in an elevation in dissolved N_2 on the order of 1% in the outlet water relative to the inlet water. Respiration in the headspace water reduced dissolved oxy-

gen to 40–60% of saturation. Turnover time of the overlying water was 6–7 h.

Dissolved gases (N_2, O_2, and Ar) in the inflow and outflow water were monitored at least once daily during the experiments. Samples were collected in triplicate in 5-ml glass test tubes to overflowing. The tubes were immediately capped by inserting the bottom end of a second tube into a Tygon tubing collar fitted snuggly on the sample tube. This inexpensive gas-tight container method reliably excluded bubbles during the capping procedure and proved free of gas leaks for >8 h in separate trials using samples heavily enriched with $^{18}O_2$. Flow rate was measured daily for each experimental chamber.

The effect of elevated nitrate concentration was determined by adding KNO_3 as a 1,000× stock solution to the inlet reservoir and (at t_0) directly to the water above the sediment in order to obtain a stepwise increase in the NO_3^- concentration above the sediment. NO_3^- concentration in the chambers was verified by direct measurement on the outlet water.

Dissolved gases were measured directly on water samples using a membrane-inlet mass spectrometer optimized for signal stability and analytical precision. Details of the instrumentation have been described elsewhere (Kana et al. 1994). The configuration of the sample introduction apparatus effectively makes the instrument serve as a high-precision dissolved gas analyzer with a throughput of ~30 samples (<5 ml) per hour. Briefly, water samples were continually pumped through a capillary-size silicone membrane located inside the vacuum inlet of a quadrupole mass spectrometer (QMS). The water-pumping system consisted of a Rainin Rabbit peristaltic pump that drew water up through a diptube in the sample and directed it through stainless steel-capillary tubing that passed through a constant-temperature heat exchanger immediately before entering the mass spectrometer vacuum. The QMS signals are proportional to the concentration of the dissolved gases in solution. We continuously monitored the three masses and calculated gas ratios in a continuous cycle until the measurement stabilized, usually within 90–120 s. In practice, the highest precision is obtained with ratio data. For this study, we used N_2:Ar and O_2:Ar ratio data, which have coefficients of variation for replicated samples of ~0.03 and ~0.05%, respectively (Kana et al. 1994). Thus, the signal-to-noise ratio for our experiments was on the order of 30:1 for ΔN_2 measurements. Instrument standardization was done frequently using air-equilibrated brackish water kept at constant temperature and humidity (Kana et al. 1994). Gas concentration was determined from equations provided by Colt (1984). Nitrate was analyzed by an Technicon AutoAnalyzer. Temperature was measured using a NIST-traceable mercury thermometer.

The net flux of N_2 by the cores was determined from the following relationship:

$$F = [(C_i - C_o)V_f/A] - F_b,$$

where C_i and C_o are the concentrations (μmol N liter^{-1}) of N_2 in the inlet and outlet of the sample cylinders, respectively, V_f is the volumetric flow rate (liters h^{-1}), A is the sediment surface area (m^2), and F_b is the N flux (μmol N m^{-2} h^{-1}) in the blank core. F_b was calculated from the flux equation above without blank correction. The O_2 flux was calculated similarly except that a scaling factor was applied to F_b. This different treatment was used because of the following rationale. We assumed that fluctuations in the N_2:Ar ratio of the blank chambers reflected variability in the inlet water only, because microbial activity with respect to N_2 was expected to be insignificant in the oxic water. On the other hand, O_2 flux in the blank cores could have occurred through microbial activity, and because the residence time in the larger head-volume blank chambers was longer than in the sample chambers, we determined the volumetric flux (substituting head volume, V, for A). This volumetric O_2 flux was then scaled down to the smaller head-volume sample chambers.

The response time of sediment denitrification was evaluated by comparing the measured change in N_2 flux to the theoretical change assuming an instantaneous response. Because there is a lag in the response of the gas concentration in the chamber associated with the residence time of the overlying water (i.e. it takes finite time to bring N_2 in the reservoir to a new steady state), the *apparent* rate during the transition is different from the final rate in steady state. In a continuous-flow system that responds by a stepwise change in rate, the apparent flux during the transition can be described by

$$(F_2 - F_1)F(t) + F_1 = 1 - e^{-t/\tau},$$

where F_2 represents the steady-state flux after, for instance, a nitrate shift-up, F_1 represents the steady-state flux before nitrate addition, t is the time after the addition (h), and τ is the turnover time (h) of the system (Brezonik 1994). If measured (apparent) rates follow the theoretical response, then the rate process changes instantaneously to the new level upon the step-up in substrate.

We conducted a sampling in early July when the nitrate level at the up-river site was >36 μM. This was approximately one-third the level typical of spring conditions and higher than what is generally observed during summer in that part of the river (Stevenson et al. 1993). Salinity, temperature, and nitrate concentration at each of the four sample sites are shown in Table 1. The salinity gradient was associated with a nonconservative gradient in nitrate. The seaward end site had 1 μM nitrate. Steady-state denitrification rates at each site, determined as the average of four consecutive daily measurements under continuous-flow conditions, were measured using ambient water to reflect in situ activity. A gradient in denitrification corresponded to the change in river water nitrate concentration between sites (Table 1). Denitrification decreased from 123 μmol N m^{-2} h^{-1} at the upstream site to ~50 μmol N m^{-2} h^{-1} downstream. Oxygen consumption ranged from 2,000 to 3,500 μmol O_2 m^{-2} h^{-1} and did not exhibit a gradient similar to the other variables.

A second sampling at the end-member locations was conducted in early August when nitrate was <1 μM across the salinity gradient (Table 1). Denitrification rates were similar at 37 and 40 μmol N m^{-2} h^{-1} for the two sites investigated. Oxygen consumption was also similar at a level of ~2,200 μmol O_2 m^{-2} h^{-1}.

The response to nitrate loading was determined by increasing the nitrate concentration in the feed water and

Table 1. Site characterization and rates of denitrification and respiration in continuous-flow experiments for the early July sampling.

Exp.	Site	Temp. (°C)	Nitrate (μM)	Salinity (ppt)	Denitrification rate (μmol N m^{-2} h^{-1})		Respiration rate (μmol O_2 m^{-2} h^{-1})	
					Before addition*	After addition*	Before addition	After addition
Jul	1	26.1	36	1.0	123	190	3,320	2,930
Jul	2	26.5	10	5.0	81	179	2,090	2,540
Jul	3	26.7	3	8.2	45	206	2,760	3,490
Jul	4	26.0	1	13.0	51	223	3,670	3,420
Aug	1	31	<1	3.9	37	132	2,180	2,140
Aug	4	30	<1	14.0	40	137	2,240	2,370

* Refers to rates determined before or after nitrate addition to the experimental chambers.

chamber water by 100 μM in a stepwise fashion after the fluxes had been in steady state for 4 d. Figure 1 shows the denitrification rates for the four sites from Exp. 1 for 4 d prior and 4 d after an experimental increase in nitrate concentration. The most significant increase in denitrification rates upon nitrate loading was associated with cores initially exhibiting low activity. In most cases the increase occurred primarily during the first 24 h. There was an indication of a slower increase in denitrification rates from days 2 through 4, particularly in samples originating from the two higher salinity sites.

A nitrate addition experiment was repeated with an emphasis on resolving the kinetics of the denitrification rate response. Figure 2 shows the response for 4 d prior and 8 d after the increase in nitrate to the cores. Sediment from the two end-member sites behaved similarly before and after the increase. During the 8-d period after nitrate loading, there was no indication of growth in the population of denitrifying bacteria as the rates came to a new steady state within the first day and remained constant thereafter. The inset of Fig. 2 shows the region surrounding the nitrate addition. The apparent rates closely followed the theoretical response calculated assuming an instantaneous increase to the new steady-state rate.

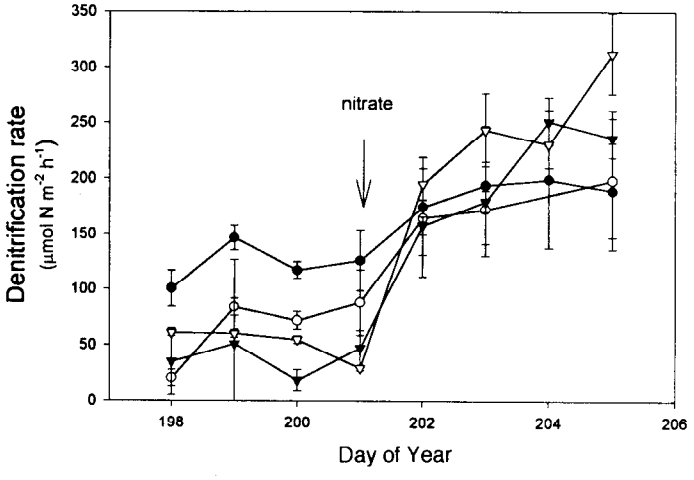

Fig. 1. Denitrification in sediment cores from four sites along a salinity gradient (*see Table 1*). Error bars represent standard errors of the mean for triplicate cores. ●, site 1; ○, site 2; ▼, site 3; ▽, site 4.

The denitrification rates for the experiments described above were pooled with data from an additional nitrate-loading test conducted during the second experiment. Rates were compared with the nitrate concentration in the overlying water. The steady-state denitrification rate was proportional to the nitrate concentration in the overlying water up to 185 μM, the maximum concentration tested (Fig. 3). The intercept at 0 nitrate was at a denitrification rate of 60 μmol N m^{-2} h^{-1}. We interpret this to be the rate supported by nitrification in the sediments.

The nitrate dependency shown in Fig. 3 indicates that water column nitrate is an important environmental control on denitrification in the Choptank River. Salinity effects, as well as other potential indirect effects that correlate with salinity, such as sulfide concentration, are at most small in comparison with the direct effect of nitrate in the overlying water. We have previously shown by using similar methodology that denitrification in brackish pond sediments can be elevated by the addition of an organic carbon source (acetate) when nitrate is present and that the denitrification rate can be co-limited by both nitrate and organic carbon (Kana et al. 1994). We did not investigate the addition of carbon

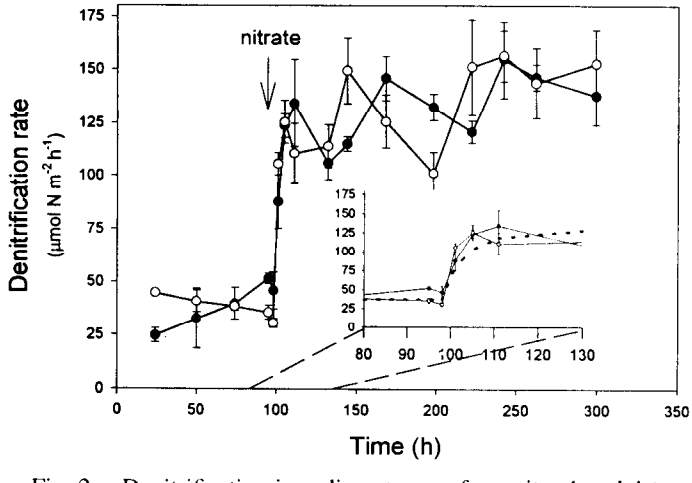

Fig. 2. Denitrification in sediment cores from sites 1 and 4 (*see Table 1*). Error bars represent standard errors of the mean for triplicate cores. ○, site 1; ●, site 4. Inset: Expansion of the region surrounding the time that nitrate was added to the experiment. The dashed line indicates changes in the apparent rate assuming an instantaneous response of denitrification.

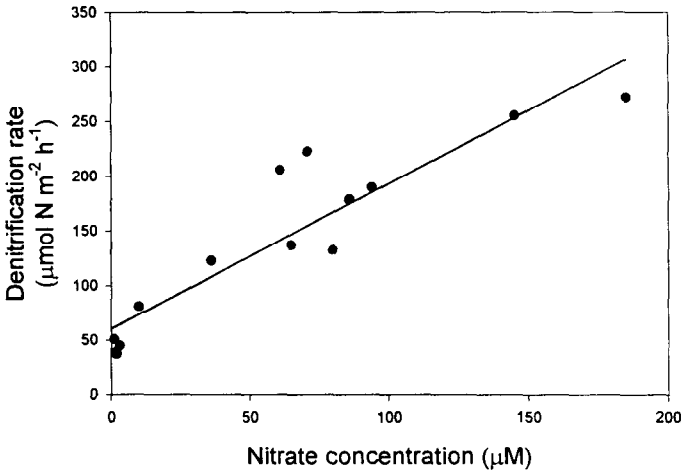

Fig. 3. Relationship between denitrification and the concentration of nitrate in the overlying water.

sources in the present study, and cannot rule out a potential carbon limitation superimposed on the nitrate limitation identified here. Nevertheless, the response of sediments from different locations on the salinity gradient was broadly similar with respect to nitrate loading. This suggests that co-limiting factors, if present, affected the process in similar ways among the samples from the different sites.

A linear relationship between nitrate concentration in the overlying water and denitrification in the sediments has been observed in several studies recently (Pelegrí et al. 1994; Seitzinger 1994; Nielsen et al. 1995). This empirical result suggests relatively simple control of denitrification by nitrate in the water column. The relationship can be represented as

$$F_N = kC_w + F_0,$$

where F_N is the denitrification rate (mmol N m^{-2} h^{-1}), k is the slope (m h^{-1}), C_w is the nitrate concentration in the water (mmol N m^{-3}), and F_0 is the baseline denitrification flux (mmol N m^{-2} h^{-1}) in the absence of nitrate in the overlying water. F_0 is likely to be due to coupled nitrification–denitrification in the sediments. A linear relationship between water-column nitrate and denitrification implies that F_0 does not change as a function of the additional nitrate source. A deviation from linearity in real systems could, in principle, be partially due to changes in the rate of coupled nitrification–denitrification, although we have no reason to think that the rate of nitrification is influenced by nitrate levels.

The slope of the relationship can provide important insight into the control of denitrification. The slope, k, has units of length per time (e.g. cm s^{-1}), which can be related to a transport coefficient. Transport of nitrate across the water–sediment interface is determined by a transport coefficient, k_t, times the nitrate concentration gradient, i.e. $F = k_t(C_w - C_s)$, with C_s being the minimal nitrate concentration in the sediment. The gradient is determined by C_w, an independent variable, and C_s, a variable that depends on the capacity of the denitrifying bacteria to remove nitrate from the sediment. Assuming a diffusion model, k_t is equal to a diffusivity coefficient, D, for the specific material (nitrate) and physical system divided by an effective path length, z, i.e. $k_t = D/z$. For a given experimental system in steady state, D, z, and therefore k_t are constant. Significantly, a linear relationship between the flux of material and the concentration of substance on the source side (C_w) is only possible when the minimum concentration is held constant. Therefore, with respect to denitrification in the experimental sediments, the observed proportionality between the denitrification flux and the concentration of nitrate in the water implies that the concentration of nitrate at the site of the denitrifers was constant. Because linearity holds at nitrate concentrations down to 1 μM, we conclude that the denitrifying bacteria effectively removed all of the nitrate in their immediate vicinity.

We calculated the slope of the denitrification–nitrate relationship from this and other studies (Table 2) to determine the range in transfer coefficients. Recognizing that these coefficients are subject to effects of temperature and other physical properties of the sediments that affect diffusion of nitrate to the sites of denitrification, we note that they span ~1 order of magnitude (i.e. 0.5×10^{-5}–6.2×10^{-5} cm s^{-1}). As a first approximation, if we assume a value of 1.5×10^{-5} cm^2 s^{-1} for the diffusivity coefficient, D, at 25°C and a porosity of 0.9 (Lerman 1979), then the effective diffusive path length for nitrate transport is 0.24–3 cm.

For the present study, the calculated diffusive path length for nitrate is close to 0.5 cm. This distance, while at the low end of the range from various studies, is of a length that would require a significant amount of time (>10 h) for nitrate to traverse. Hence, there is a contradiction with respect to the observation of an apparently immediate response of denitrification to a sudden increase in nitrate and the time required for nitrate to diffuse to the sites of denitrification and for N_2 to diffuse out to the water column for measurement. We think that our method could have resolved a lag

Table 2. Transfer coefficients for nitrate moving from the water to the sites of denitrification in sediments. Coefficients are calculated from the slope of the denitrification vs. nitrate concentration relationship (*see text*).

Reference	Transfer coefficient (cm s^{-1})	Notes
This study	3.6×10^{-5}	Estuarine sediment, 25°C
Nielsen et al. 1995	0.56×10^{-5}	Estuarine sediment, pooled data from seasonal study, 0–25°C
Pelegrí et al. 1994	3.9×10^{-5}	Estuarine sediment, 13°C, 20×10^3 amphipods m^{-2}
	1.1×10^{-5}	Estuarine sediment, 13°C 0 amphipods m^{-2}
Seitzinger et al. 1993	6.3×10^{-5}	Lake sediment, 23°C
Seitzinger 1994	3.6×10^{-5}	Heath wetland saturated soil, 23°C
	0.8×10^{-5}	Cedar swamp saturated soil, 23°C

caused by the time constraints of the diffusion process if the path length was as estimated. We also note that the 0.5-cm path for denitrification estimated by the present model is considerably greater than the predicted depth of the oxic layer. By using the relationship described by Cai and Sayles (1996) with an average oxygen flux rate and water-column concentration from our experiments, the expected depth of oxygen penetration was ~0.05 cm, or an order of magnitude shallower than the depth of denitrification. The apparent difference in the depth of the two layers is inconsistent with indications of the denitrification zone being in close proximity to the base of the oxic layer or above (Brandes and Devol 1995).

It is possible that the rapid response of denitrification to sudden changes in water-column nitrate reflects a shallower distribution of denitrification zones than that estimated by the simple diffusion model applied here. A one-dimensional diffusion model assumes that the microbially mediated processes are uniform horizontally. If that is not the case and there were heterogeneously displayed "hot-spots" of denitrification activity (Brandes and Devol 1995), then the actual areal flux rate of the hot-spots would be higher than the measured rate averaged over the surface area of the core. For example, if the actual diffusive layer thickness for denitrification, z_d, was 0.05 cm (the oxygen penetration depth), then the hot-spots would cover 10% of the surface area of the core (i.e. the unit area flux is scaled 10 times higher). The importance of A in the calculation of z_d for the putative denitrification zones is apparent from this analysis, but its direct measurement is not yet possible.

This simple diffusion model, despite its limitations, may be of use for analyzing sediment denitrification responses to other environmental factors. The relatively constant sediment oxygen demand observed in our study suggests that the sediments exhibited a relatively constant oxygen penetration depth. If that depth constrains the denitrification depth, then we would expect z_d to be constant and there would be a linear relationship between denitrification rate and nitrate loading, which we observed. In a previous study (Kana et al. 1994), we added acetate to steady-state pond-sediment cores after adding nitrate. Additions of nitrate followed by nitrate + acetate stimulated the denitrification rate in succession. This apparent co-limitation by oxidant and reductant may be explained by a reduction in the oxygen penetration depth caused by an increase in sediment oxygen demand after the addition of acetate (unpubl. data). By this putative mechanism, acetate stimulates denitrification by reducing z_d, which increases k_t and the efficiency of nitrate transport to denitrifiers.

Regardless of the underlying mechanism, it is apparent from our experiments that denitrification responded rapidly in an environmental context to increases in nitrate in the overlying water. Environmental fluctuations in nitrate in the water column can occur at frequencies of tidal excursions or slower. Moore et al. (1996) measured fluctuations in nitrate of between 2 and 10 μM on a timescale of hours in the Choptank River in June at a location near our site 4. The kinetic results described here indicate that sediment denitrification tracks such fluctuations quite closely. A rapid response by denitrifying bacteria has also been noted in intertidal mud flats (Joye and Paerl 1993). In terms of modeling environmental denitrification, the correlation of denitrification to water-column nitrate is simplified because of such tight coupling.

The tight coupling indicates that the denitrifying bacteria were poised to utilize nitrate when it became available. In the August dataset, there was little or no change in denitrification rate under conditions of high nitrate loading for a period of 10 d. This was surprising considering that it apparently reflected a 2–3-fold increase in respiration and, by implication, growth of the population of denitrifying bacteria. The lack of a populational response may indicate that the denitrifying bacteria under conditions of low nitrate availability were not physiologically limited by a shortage in nitrate as the respiratory electron acceptor. Rather, the denitrifying bacteria may have been utilizing (an) alternative electron acceptor(s) (e.g. iron) during periods of low nitrate availability (e.g. Sørensen 1982). With an increase in available nitrate, a shift in electron acceptors may have occurred without a significant change in respiratory electron transport.

In conclusion, our results indicate that denitrification in brackish water sediments was directly affected by the transport flux of nitrate from the water column to the sediments and that the denitrifying bacteria remained poised to utilize nitrate as a respiratory electron acceptor. The rapid response of denitrification facilitates modeling the ecological process because it does not require a time lag or damping term.

Todd M. Kana
Matthew B. Sullivan
Jeffrey C. Cornwell
Kevin M. Groszkowski

Horn Point Environmental Laboratory
P.O. Box 775
Cambridge, Maryland 21613

References

BRANDES, J. A., AND A. H. DEVOL. 1995. Simultaneous nitrate and oxygen respiration in coastal sediments: Evidence for discrete diagenesis. J. Mar. Res. **53:** 771–797.

BREZONIK, P. L. 1994. Chemical kinetics and process dynamics in aquatic systems. CRC Press.

CAI, W.-J., AND F. L. SAYLES. 1996. Oxygen penetration depths and fluxes in marine sediments. Mar. Chem. **52:** 123–131.

COLT, J. 1984. Computation of dissolved gas concentrations in water as functions of temperature salinity and pressure. Am. Fish. Soc. Spec. Publ. **14.**

JENKINS, M. C., AND W. M. KEMP. 1984. The coupling of nitrification and denitrification in two estuarine sediments. Limnol. Oceanogr. **29:** 609–619.

JOYE, S. B., AND H. W. PAERL. 1993. Contemporaneous nitrogen

Acknowledgments

This paper was improved through comments and insight from an anonymous reviewer. This work was supported by REU awards to M.B.S. and K.G. through a NSF and MD Sea Grant. Additional support was provided by the U.S. EPA Multiscale Experimental Ecosystem Research Center to T.M.K. and J.C.C. This is contribution 3050 from the Center for Environmental Studies of the University System of Maryland.

fixation and denitrification in intetidal microbial mats: Rapid response to runoff events. MEPS **94:** 267–274.

KANA, T. M., C. DARKANGELO, M. D. HUNT, J. B. OLDHAM, G. E. BENNETT, AND J. C. CORNWELL. 1994. A membrane inlet mass spectrometer for rapid high precision determination of N_2, O_2, and Ar in environmental water samples. Anal. Chem. **66:** 4166–4170.

KEMP, W. M., P. SAMPOU, J. CAFFREY, M. MAYER, K. HENRIKSEN, AND W. R. BOYNTON. 1990. Ammonium recycling versus denitrification in Cheasapeake Bay sediments. Limnol. Oceanogr. **35:** 1545–1563.

LERMAN, A. 1979. Geochemical processes in water and sediment environments. Wiley.

MOORE, K. A., AND OTHERS. 1996. Chesapeake Bay nutrients, light and SAV: Relationships between water quality and SAV growth in field and mesocosm studies. U.S. EPA Tech. Rept.

NIELSEN, K., L. P. NIELSEN, AND P. RASMUSSEN. 1995. Estuarine nitrogen retention independently estimated by the denitrification rate and mass balance methods: A study of Norsminde Fjord, Denmark. Mar. Ecol. Prog. Ser. **119:** 275–283.

PELEGRÍ, S. P., L. P. NEILSEN, AND T. H. BLACKBURN. 1994. Denitrification in estuarine sediment stimulated by the irrigation activity of the amphipod *Corophium volutator*. Mar. Ecol. Prog. Ser. **105:** 285–290.

RYSGAARD, S. N. RISGAARD-PETERSEN, N. P. SLOTH, K. JENSEN, AND L. P. NIELSEN. 1994. Oxygen regulation of nitrification and denitrification in sediments. Limnol. Oceanogr. **39:** 1643–1652.

SEITZINGER, S. P. 1988. Denitrification in freshwater and coastal marine ecosystems: Ecological and geochemical significance. Limnol. Oceanogr. **33:** 702–724.

———. 1994. Linkages between organic matter mineralization and denitrification in eight riparian wetlands. Biogeochemistry **25:** 19–39.

———, L. P. NIELSEN, J. CAFFREY, AND P. B. CHRISTENSEN. 1993. Denitrification measurements in aquatic sediments: A comparison of three methods. Biogeochemistry **23:** 147–167.

SØRENSEN, J. 1982. Reduction of ferric iron in anaerobic marine sediment and interaction with reduction of nitrate and sulfate. Appl. Environ. Microbiol. **43:** 319–324.

STEVENSON, J. C., L. W. STAVER, AND K. W. STAVER. 1993. Water quality associated with survial of submersed aquatic vegetation along an estuarine gradient. Estuaries **16:** 346–361.

Received: 24 January 1997
Accepted: 20 May 1997

Limnol. Oceanogr., 43(2), 1998, 339–347

Factors potentially preventing trophic cascades: Food quality, invertebrate predation, and their interaction

Abstract—Recent laboratory work on food quality constraints on zooplankton growth and reproduction, as well as several examples of weak effects of food-web manipulations on lower trophic levels in lakes with phosphorus-deficient phytoplankton, suggests that food quality effects may have currently unappreciated effects on zooplankton success and food-web interactions under field conditions. We experimentally manipulated two factors that we anticipated might play a role in suppressing *Daphnia* in P-limited lakes—the quality of phytoplankton food and the presence of the invertebrate predator *Chaoborus punctipennis*. We used a two-factor design, manipulating food source and presence of *Chaoborus*, and measured growth rate, survivorship, and fecundity of *Daphnia rosea* neonates incubated at fixed food levels in flow-through growth chambers. *D. rosea* grew significantly faster and was significantly more fecund when fed seston from a high-food quality lake (Lake 979) relative to a treatment fed seston from a low-food quality lake (Lake 110). *Chaoborus* reduced survivorship of *D. rosea* but the food source–predator interaction term was not significant, indicating that invertebrate predation and phytoplankton food quality did not influence *Daphnia* populations synergistically in this experiment. A second experiment was conducted to determine if variation in *Daphnia* growth rate and fecundity when fed food of varying quality was caused by a change in feeding rate. *Daphnia* feeding rate increased with improved food quality, suggesting that *Daphnia* responds to increases in food quality, at least in part, by increasing feeding rate. We conclude that food quality can strongly affect *Daphnia* feeding, growth, and reproduction, thereby constraining food-web dynamics in nutrient-deficient lakes.

Trophic cascades have been well documented in the literature (Shapiro and Wright 1984; Carpenter et al. 1987; Northcote 1988; Carpenter and Kitchell 1992, 1993), and even skeptics of the generality of top-down effects conclude that reduction in planktivore density after introduction of piscivores routinely increases zooplankton abundance and(or) mean size (McQueen 1990; DeMelo et al. 1992). Usually the increase in zooplankton size results from an increase in the proportion of *Daphnia* in the zooplankton community (Brooks and Dodson 1965; Shapiro et al. 1975; Hall et al. 1976; Carpenter et al. 1985). However, several recent lines of evidence indicate that the full range of response of lake food webs to manipulation of top predators may also be constrained at the level of the zooplankton–phytoplankton interaction. A number of laboratory studies have appeared indicating the possibility of strong food quality effects on zooplankton growth and reproduction. In particular, it has been shown that growth and reproduction of *Daphnia* are severely depressed when *Daphnia* feeds on P-limited algae having a high C:P ratio (Urabe and Watanabe 1992; Sommer 1992; Sterner 1993; Sterner et al. 1993). This sensitivity may reflect the high somatic P requirement of *Daphnia* (Andersen and Hessen 1991). Because *Daphnia* is considered by many workers to be central to a strong trophic cascade (Carpenter et al. 1985; Stockner and Porter 1988; de Bernardi and Giussani 1990; Gulati et al. 1990; Reynolds 1994), the possibility exists that effects of upper trophic levels may not